AD-A131 798 STUDY OF VIBRATIONAL ENERGY TRANSFER AT A SURFACE BY A 1/1
TIME-OF-FLIGHT METHOD(U) WASHINGTON UNIV SEATTLE DEPT
OF CHEMISTRY W YUAN ET AL. 31 JUL 83 NR092-549-TR27
UNCLASSIFIED N00014-75-C-0690 F/G 7/3 NL

END
FILMED
DTIC

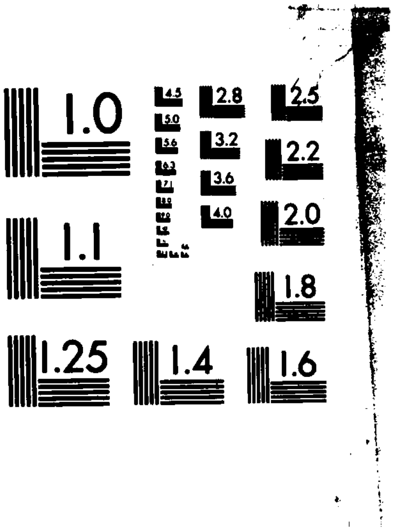

MICROCOPY RESOLUTION TEST CHART
NATIONAL BUREAU OF STANDARDS-1963-A

ADA131798

(12)

Study of Vibrational Energy Transfer at a Surface by a Time-of-Flight Method

Wei Yuan and B. S. Rabinovitch

Department of Chemistry BG-10. University of Washington
Seattle, Washington 98195

Technical Report No. NR092-549-TR27

Contract N00014-75-C-0690, NR-092-549

July 31, 1983

OFFICE OF NAVAL RESEARCH
Department of the Navy Code 432
800 N. Quincy
Arlington, VA 22217

DTIC
ELECTE
AUG 24 1983
S D
E

83 08 24 023

Unclassified

SECURITY CLASSIFICATION OF THIS PAGE (When Data Entered)

REPORT DOCUMENTATION PAGE

READ INSTRUCTIONS BEFORE COMPLETING FORM

1. REPORT NUMBER NR092-549-TR27

2. GOVT ACCESSION NO. AD-A131 798

3. RECIPIENT'S CATALOG NUMBER

4. TITLE (and Subtitle) Study of Vibrational Energy Transfer at Surface by a Time-of-Flight Method

5. TYPE OF REPORT & PERIOD COVERED Technical

6. PERFORMING ORG. REPORT NUMBER

7. AUTHOR(s) W. Yuan and B. S. Rabinovitch

8. CONTRACT OR GRANT NUMBER(s)
NR0014-75-C-0690
NR092-549

9. PERFORMING ORGANIZATION NAME AND ADDRESS
Professor B. S. Rabinovitch
Department of Chemistry, BG-10
University of Washington, Seattle, WA 98195

10. PROGRAM ELEMENT, PROJECT, TASK AREA & WORK UNIT NUMBERS

11. CONTROLLING OFFICE NAME AND ADDRESS
Dr. Richard Miller
Office of Naval Research, Code 432
Department of the Navy
800 N. Quincy, Arlington, VA 22217

12. REPORT DATE July 31, 1983

13. NUMBER OF PAGES 18

14. MONITORING AGENCY NAME & ADDRESS(if different from Controlling Office)

15. SECURITY CLASS. (of this report)

15a. DECLASSIFICATION/DOWNGRADING SCHEDULE

16. DISTRIBUTION STATEMENT (of this Report)
This document has been approved for public release; its distribution is unlimited.

17. DISTRIBUTION STATEMENT (of the abstract entered in Block 20, if different from Report)
To be published

18. SUPPLEMENTARY NOTES

19. KEY WORDS (Continue on reverse side if necessary and identify by block number)

Accomodation coefficient	Time-of-flight
Cyclobutene	Transition Probabilities
Energy Transfer	Unimolecular Reaction
High Temperature	Vibrational Relaxation
Surfaces	

20. ABSTRACT (Continue on reverse side if necessary and identify by block number)

→ A single collision, time-of-flight extension of the VEM method for the study of molecule-surface vibrational energy transfer is introduced. This refined technique helps election between possible alternative trial analytic forms of the collisional transition probability function. A gaussian form is preferred over a boltzmann-exponential form for cyclobutene isomerization to 1,3-butadiene energized by collisions at a seasoned silica surface at 800 K. The study illustrates the difference between conventional accomodation coefficient measurements, which examine average energy changes, and the present studies which explore the

DD FORM 1 JAN 73 1473 EDITION OF 1 NOV 65 IS OBSOLETE
S/N 0102-LF-014-6601

Unclassified

SECURITY CLASSIFICATION OF THIS PAGE (When Data Entered)

~~(20.)~~ energy transport at high levels corresponding to chemical reaction thresholds.

Study of Vibrational Energy Transfer at a Surface
by a Time-of-Flight Method[*]

Wei Yuan[†] and B. S. Rabinovitch
Department of Chemistry BG-10
University of Washington
Seattle. WA 98195

Abstract

A single collision, time-of-flight extension of the VEM method for the study of molecule-surface vibrational energy transfer is introduced. The technique helps election between possible alternative trial analytic forms of the collisional transition probability function. A gaussian form is preferred over a boltzmann-exponential form for cyclobutene isomerization to 1,3-butadiene energized by collisions at a silica surface at 800 K.

INTRODUCTION

Vibrational energy transfer during collisions of a thermal distribution of gas molecules with a solid surface is a subject of current interest. A variety of substrate molecules have been examined on various surfaces including fused silica [1,2], pyrex glass [3], polycrystalline iron [4], platinum [5] and gold [6]. Some of the work [2,4,5] concerns measurements of vibrational accomodation coefficients, i.e., probes the lower end of the vibrational energy distribution resulting from collision. The work in this laboratory [1,3,6] has dealt with vibrational excitation of substrate molecules to levels above the unimolecular reaction threshold E_0 ($\approx$30-65 kcal mole^{-1}). In this case, E_0 acts as the absorbing barrier postulated in the original random walk treatment of Rubin and Shuler [7].

The surfaces used in the work cited above are not "clean", being rapidly covered at the substrate pressures employed. In particular, they are deliberately "seasoned" at high temperatures in our work; the seasoned surface is ostensibly covered with a graphitic polymeric layer whose nature may be related to those described by Somorjai, et al [8]. However, the nature of the underlying matrix, e.g. whether gold or silica, may continue to influence the nature of the layer formed by surface treatment and its energy transfer properties [6].

The variable encounter method (VEM) used in this laboratory has been described in detail [1], including the single collision variant thereof [3]. In general, cold molecules thermalized at some lower temperature are permitted to collide with a heated surface, called the "reactor". In fitting the observed energy transfer results of VEM studies, various trial analytic forms of the collisional transition probability matrix $\underset{\sim}{P}$ have been used [1,3,9]. Prominent among these have been Exponential (E), Gaussian (G) and Boltzmann-exponential (BE) forms; the elements of the latter two obey the following relations for down-transitions (energy loss) by the molecule:

$$p^G(\Delta E) = C \exp[-(\Delta E-\Delta E_{mp})^2/2\sigma^2] \qquad (1)$$

where $\Delta E = E_j - E_i$ ($E_j > E_i$); ΔE_{mp} is the most-probable transition; σ is the standard deviation; C is a normalization constant;

$$p^{BE}_{i\leftarrow j}(\Delta E, T_h) = C\ B_i \exp(-\Delta E/\langle\Delta E\rangle) \qquad (2)$$

where $B_i = g_i \exp(-E_i/RT_h)$ is a Boltzmann weighting, T_h being the hot reactor surface temperature; $\langle\Delta E\rangle$ is an average energy transfer parameter; normalization extends over all energies, and up-transition probabilities are found by detailed balance. It transpires that several transition probability models will often fit a particular range of results although the E form has been found more apt for weaker collisions, and the G form for stronger collisions; the BE form will obviously approach the strong collision limit when $\langle\Delta E\rangle$ becomes very large.

In an attempt to distinguish better the suitability of various models, Arakawa, et al [9] studied single collision excitation of cyclobutene isomerization on a hot seasoned silica surface maintained at various temperatures and varied the initial vibrational energy, i.e., the initial (cold) temperature T_0 of the substrate, from 273 K to 600 K. Although the E model could be ruled out, both the G and BE models gave reasonable fit to the data taken at silica surface "reactor" temperatures from 600 K to 900 K (see Fig. 3 of ref. 9a). However, as may be seen from Fig. 1 (for reactor temperature 800 K), these two models make different predictions concerning both the magnitude of the accomodation coefficients α ($\alpha^G \lesssim 1$; $\alpha^{BE} < 1$), and the form of the population distribution above E_0. After a single collision the new population vector is given by $\underset{\sim}{N}^1 = \underset{\sim}{P}\ \underset{\sim}{N}^0$, where N^0 is the initial Boltzmann vector corresponding to the original (cold) temperature. (For a strong collider, $\underset{\sim}{N}^1$ becomes $\underset{\sim}{N}^h$, the Boltzmann distribution at the reactor (hot) temperature.) If $\underset{\sim}{P}$ is partitioned at E_0, i.e., $\underset{\sim}{P} = \begin{bmatrix} P_1 & P_2 \\ P_3 & P_4 \end{bmatrix}$, then obviously the reaction probability per collision P_c depends only on $\underset{\sim}{P}_3$, i.e., up-transition probabilities terminating above E_0. By contrast, measurement of α gives information only about $\underset{\approx}{E}_1$. At lower energies, $\underset{\approx}{N}_G{}^1$ follows the equilibrium population curve $\underset{\approx}{N}^h$ quite closely (hence $\alpha^G \approx 1$), while $\underset{\approx}{N}_{BE}{}^1$ drops markedly below $\underset{\approx}{N}^h$ (hence $\alpha^{BE} < 1$). Above E_0, $\underset{\approx}{N}_G{}^1$ declines more rapidly than $\underset{\approx}{N}_{BE}{}^1$. This difference in slope provides a basis for an experimental test of the relative validity of the two models. Unfortunately, as may be seen from Fig. 2, this difference in slope above E_0 is greatly reduced at lower reactor temperatures so that in this system it provides an adequate basis for experiment only at the highest temperature employed here, 800 K. By changing the flight distance between the hot surface and a cold wall, the flight time τ during which decomposition may take place can be altered. Since the specific decomposition probability k(E) varies with energy in a range of operational accessibility (Fig. 1), i.e., $k^{-1}(E) \approx O(\tau)$, it is possible to probe the form of $\underset{\approx}{N}^1$. It may be assumed [3,9,10] that accomodation of cyclobutene on a cold (≈285K–330K) surface is complete in one collision so that partial cooling and multiple reflection is not a problem.

Experimental

Cyclobutene was obtained from Columbia Chemicals, >99.9%. It was further purified by gas chromatography.

The reactor (Fig. 3) consisted of a 1-l spherical pyrex flask provided with an internally-heated lathe-aligned central silica cylinder finger having a flat ground fused silica end H positioned at the center of the flask. The thin ground silica flat (diam. 3 cm) constituted the hot surface. The internal cylinder was described previously [3] and was a thermostatted liquid metal bath, B. The wall of the cylinder was double jacketed and cooled. Facing the silica flat was an overlapping flat brass surface C which was the end of a water cooled cylinder that moved smoothly on a screw S with a no-twist, no-play action and pumped O-ring seals, O. The flight distance between flats was changed from 0.02 cm to 5.6 cm. Temperature measurements were made with two chromel-alumel thermocouples which dipped into the liquid metal alloy inside the finger. The temperature of the hot bath was varied from 550-820 K. The hot silica surface was seasoned with cyclobutene ($\approx 3 \times 10^{-4}$ torr) at 800 K for one hour. The reaction pressure was $0.8-1 \times 10^{-4}$ torr, so the system was at the second order region. Cyclobutene isomerizes to 1,3-butadiene. No by-product was found on a FID chromatographic system. Every experimental point shown in Fig. 4 was the average of three to four separate measurements. Samples were admitted to the flask for a period of time that produced 1-5% reaction usually. Analysis was made on a SCOT squalane column or on a 3/16" packed squalane column on Chromosorb P.

Results and Calculations

Four average flying distances were tested: 0.046, 0.126, 0.32 and 5.6 cm. For the former three distances, the temperature of the cold brass surface was ≈285 K. For the longest distance (the finger completely retracted), the wall of the flask was heated slightly by the hot surface and was maintained at ≈320 K. This made a slight change in the number of collisions at given pressure with the hot surface, and in the initial Boltzmann distribution. The latter effect is slight and could readily be reduced to 285 K by use of the measurements in ref. 9a.

As before [10], the unimolecular reaction obeyed the first order law with respect to time. From the experimental rate constant k, the reaction probability per collision P_c is given by (Appendix A), $P_c = 4kV/ca$, where V is the volume of the reactor; a is the area of the hot surface; c is the average speed of the molecules. A P_c vs. T_h plot is shown in Fig. 4. The plot of P_c vs. flight distance, d, is given in Fig. 5 for $T_h = 800$ K.

P_c values were also calculated by computer simulation.

$$P_c = \int_{E_0}^{\infty} N^1(E,T)\left[1-e^{-k(E)\tau(d,T)}\right]dE \Big/ \int_0^{\infty} N^1(E,T)dE$$

k(E) is the microscopic rate constant according to RRKM theory; $\tau(d,T)$ is the flight time; d is the average flight distance. By fitting Fig. 4, the parameters $\langle \Delta E \rangle$ and ΔE_{mp} to be used in $\underset{\sim}{P}$ in order to generate $\underset{\sim}{N}^1$ were deduced at several temperatures over the range used. In Table 1 are given resulting values of $\langle \Delta E^1 \rangle$, the average down-jump step, and α, for the two models under consideration. Calculated plots of P_c are compared with experiment at 800 K in Fig. 5.

RRKM values of k(E) shown in Fig. 1 were calculated with use of activated complex model A given by Elliot and Frey [11]. Their complex C has also been used but does not give as good concordance; this is considered further below. The frequencies used for the molecule and complex are tabulated in Appendix B.

Discussion

Reference to Table 1 reveals reasonable concordance between the values of this study and the values of ref. 9a for both the average down-step size, $<\Delta E^1>$, and the vibrational accomodation coefficients, α.

The G and BE models when compared with experiment in the plot of P_c vs. T in Fig. 5 reveal better concordance for the former model. Both calculations were adjusted by a few percent so as to fit the 800 K data. The absolute values of k(E) are sensitive to the choice of activated complex models, and thus also is the goodness of fit of calculated values to experiment. Use of activated complex C of Elliot and Frey would not give as good absolute agreement but, nevertheless, model G still gives relatively better concordance than does model BE. We conclude that the gaussian collisional transition probability model is the preferred one and that, on silica, vibrational accomodation coefficient values close to unity are also favored.

The only comparable data are those of ref. 2 for octane on fused silica for which intermediate values (≈0.5) were reported in measurements made at lower vibrational energies, well below reaction threshold values. Since octane is a higher boiling species, with a larger Lennard-Jones force constant than cyclobutene, a smaller α value is not expected. The discrepancy may suggest an energy transfer model intermediate between the two tested here. Our use of models such as E, G, etc., now and in the past, has been simply as pragmatic analytic forms having somewhat different properties and differing physical connotations [12]. There is an urgent need for the efforts of theoreticians to make the admittedly difficult connections with solid state and molecular properties and potentials and with eigenstate densities. This need exists also because of the practical importance of thermal high-energy phenomena.

The fit of calculations to experiment (not shown) is not as good at 700 K and 600 K, although the G model continues to be preferred. As mentioned earlier, the operational distinction between the two models decreases, but another difficulty is the heavier and irregular dependence of k(E) on the complex model details at lower temperature and energies where k(E) ceases to behave as a smooth monotonic function of E. This difficulty would be minimized in the examination of larger molecules having more, and more-dispersed, vibrational frequencies, and with a consequent wider range of energies probed above E_0 at given temperature - apart from any fundamental difficulties of the rate theory at energies near the reaction threshold [13]. Decomposition, rather than isomerization systems would be more favored in order to keep values of k(E) up in the experimentally accessible range.

Table I. Average energy transfer down-step $\langle \Delta E^{1} \rangle$ (cm^{-1}) and vibrational accomodation coefficient α in the single-collision cyclobutene system.[a]

T_h (K)	Model	$\langle \Delta E^{1} \rangle$	α
800	G	4330 (4100)[b]	0.95 (0.94)[c]
700		4940 (4200)	0.98 (0.97)
600		5550 (5640)	0.96 (0.96)
800	BE	4230 (3500)	0.26 (0.20)
700		5590 (4450)	0.33 (0.24)
600		6580 (6400)	0.38 (0.33)

[a] For an initial temperature T_0 of 285 K.

[b] Parenthetic values are average values from ref. 9a for initial temperatures over the range 273 K - 600 K.

[c] Values from ref. 9a for initial temperature of 273 K.

Appendix A: The calculation of collision rate and P_c values.

When the flight distance is long, the collision rate with the hot surface is obviously governed by the flask temperature, T_0. If the flight distance is only several millimeters or less, the speed distribution of the molecules inside the hot-cold gap is influenced by the temperature of the hot surface. A one-dimensional approximation is suitable for our case. A "reduced" temperature, $T_m^{1/2} = 2(T_h T_0)^{1/2} / [(T_h)^{1/2}+(T_0)^{1/2}]$, should ostensibly be used [14] instead of T_0 to estimate the collision rate. However, the usual equation for calculating the P_c values from the observed rate constant k is still correct in this case. When the steady state is established, $N_g c_g = N_f c_f$, where N_g is the concentration of the gas inside the gap; c_g is the average speed of the gas inside the gap; $c_g = (8RT_m/\pi M)^{1/2}$; N_f is the concentration of the gas outside the gap; c_f is the average speed of the gas outside the gap, $c_f = (8RT_0/\pi M)^{1/2}$.

Inside the gap one has the usual equation for calculating P_c: $P_c = 4k_g V_g / c_g a$; where k_g is the "real" rate constant of this isomerization reaction inside the gap; V_g is the volume of the gap; a is the area of the hot surface. In our experiment P_c is equal to or less than 10^{-4} and the composition of the gas inside the gap is the same as the composition of the gas outside. The quantity actually measured is the total rate constant k based on the whole flask. Then, $k = k_g V_g N_g / (V_f N_f + V_g N_g)$; or $k_g = k[V_f (T_m/T_0)^{1/2} + V_g]/V_g$ and $P_c = 4k[V_f (T_m/T_0)^{1/2} + V_g](T_0/T_m)^{1/2}/c_f a$.

Because V_f is much bigger than V_g, $P_c = 4kV_f / c_f a$.

One further addendum. The distance between hot and cold surfaces, ℓ, is not the average flight distance, d. Assuming a cosine desorption law, then

$$d = \int_0^{2\pi}\int_0^{\pi/2} \ell \sin\theta \, d\theta \, d\phi \Big/ \int_0^{2\pi}\int_0^{\pi/2} \cos\theta \sin\theta \, d\theta \, d\phi = 2\ell$$

Appendix B: Vibrational Assignment [11]

Molecule (cm^{-1}) = 3058, 3126, 2916, 2955(2), 2933, 1566, 1444, 1426, 1288, 1276, 1210, 1182, 1113, 1100, 1074, 986, 875, 850, 846, 800, 640, 635, 325.

Activated Complex A (cm^{-1}): 3040, 3030, 3020, 3010, 3000, 2990, 1370, 1360, 1350, 1340, 1330, 1320, 1310, 1032, 1020, 1010, 1000, 990, 980, 680, 670, 660, 335.

E_0 = 32.0 kcal mol^{-1}. Reaction path degeneracy = 1.

References

* Work supported by the Office of Naval Research.

† Permanent address: Department of Chemistry and Chemical Engineering, Qinghua University, Beijing 100084, P.R. of China.

[1] Kelley, D.F.; Zalotai, L.; Rabinovitch, B.S. Chem. Phys. 46 (1980) 379.

[2] Amorbieta, V.T.; Colussi, A.J. J. Phys. Chem. 86 (1982) 3058.

[3] Kelley, D.F.; Kasai, T.; Rabinovitch., B.S. J. Phys. Chem. 85 (1981) 1100.

[4] Draper, C.W.; Rosenblatt, G.M. J. Chem. Phys. 69 (1978) 1465, and later work.

[5] Foner, S.N.; Hudson, R.L. J. Chem Phys. 75 (1981) 4727.

[6] Yuan, W.; Rabinovitch, B.S. J. Phys. Chem., in press.

[7] Rubin, R.J.; Shuler, K.E. J. Chem. Phys. 25 (1956) 59, 68.

[8] Koestner, R.J.; VanHove, M.A.; Somorjai, G.A. J. Phys. Chem. 87 (1983) 203.

[9] a) Arakawa, R.; Kelley, D.F.; Rabinovitch, B.S. J. Chem. Phys. 76 (1982) 2384;
b) Arakawa, R.; Rabinovitch, B.S. J. Chem. Phys. 86 (1982) 4772.

[10] Flowers, M.C.; Wolters, F.C.; Kelley, D.F.; Rabinovitch, B.S. Chem. Phys. Lett. 69 (1980) 543; Wolters, F.C.; Flowers, M.C.; Rabinovitch, B.S. J. Phys. Chem. 85 (1981) 589.

[11] Elliot, C.S.; Frey, H.M. Trans. Faraday Soc. 1966, 62, 395.

[12] Tardy, D.C.; Rabinovitch, B.S. Chem. Rev. 77 (1977) 369; J. Chem. Phys. 45 (1966) 3720.

[13] Schranz, H.W.; Nordholm, S.; Hamer, N.D. Intl. J. Chem. Kinet. 14 (1982) 543.

[14] Edwards, D.K.; Denny, V.E.; Mills, A.F. "Transfer Processes", McGraw-Hill Book Co., (1976) p. 154.

Captions

Fig. 1. Vibrational energy populations for cyclobutene for the reaction condition (800, 285). — — — is the thermally equilibrated Boltzmann population at 800 K; — · —, the Boltzmann population at the temperature 285 K; ——, $\underset{\sim}{N}_{BE}^{1}$ is the population vector after a single collision for the Boltzmann exponential model; — ·· —, N_G^1 is the population vector after single collision according to the Gaussian model. k(E) is also shown in this Figure. $E_0 = 11{,}203\ \mathrm{cm}^{-1}$.

Fig. 2. Vibrational energy populations for cyclobutene for the reaction condition (600, 285). Same notation as in Fig. 1.

Fig. 3. Schematic of apparatus showing hot H and cold C surfaces; internal bath, B, fitted with heater, stirrer, thermocouple wells and heat baffle, cooled triple wall. The opposing water-cooled brass surface C entered via pumped O-ring seal space, O, on a screw action, S, that permitted 7 cm of travel. G is a pyrex/quartz graded seal and M a quartz/stainless steel transition. V are spaced viewing ports for distance calibration.

Fig. 4. The reaction probability per collision P_c vs. temperature. □, △, ○, ▽ refer, respectively, to the average flight distance 5.6, 0.32, 0.126 and 0.046 cm; — — — is the strong collider curve ($E_0 = 32.0$ kcal mole^{-1}).

Fig. 5. P_c vs. d (log scale) at 800 K; ○ , experimental points; ——, Gaussian; — — — Boltzmann exponential calculations.

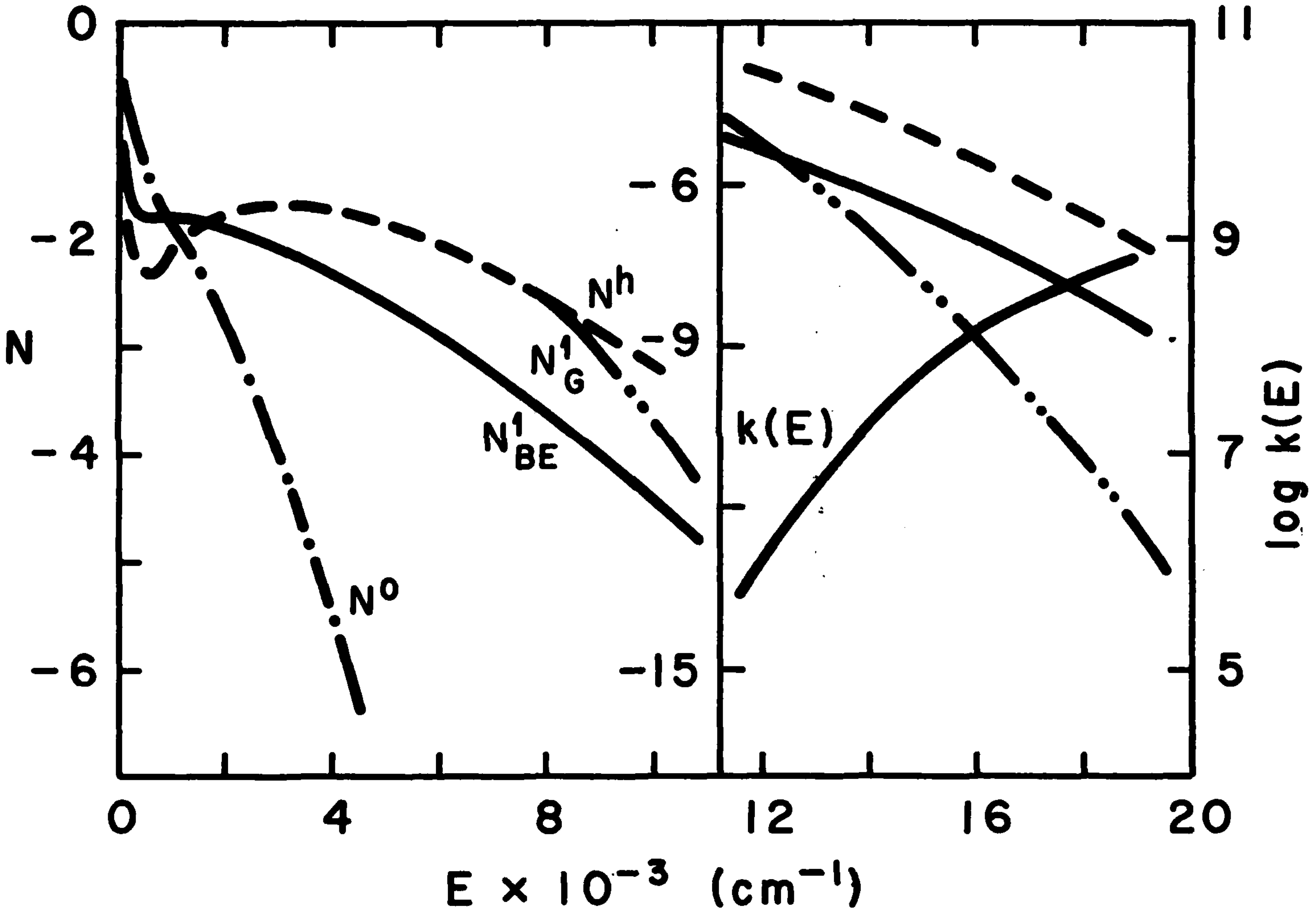
0
-2
-4
-6
N
0
4
8
12
16
20
E × 10^{-3} (cm^{-1})
-6
-9
-15
11
9
7
5
log k(E)
N^h
N^1_G
N^1_{BE}
N^0
k(E)

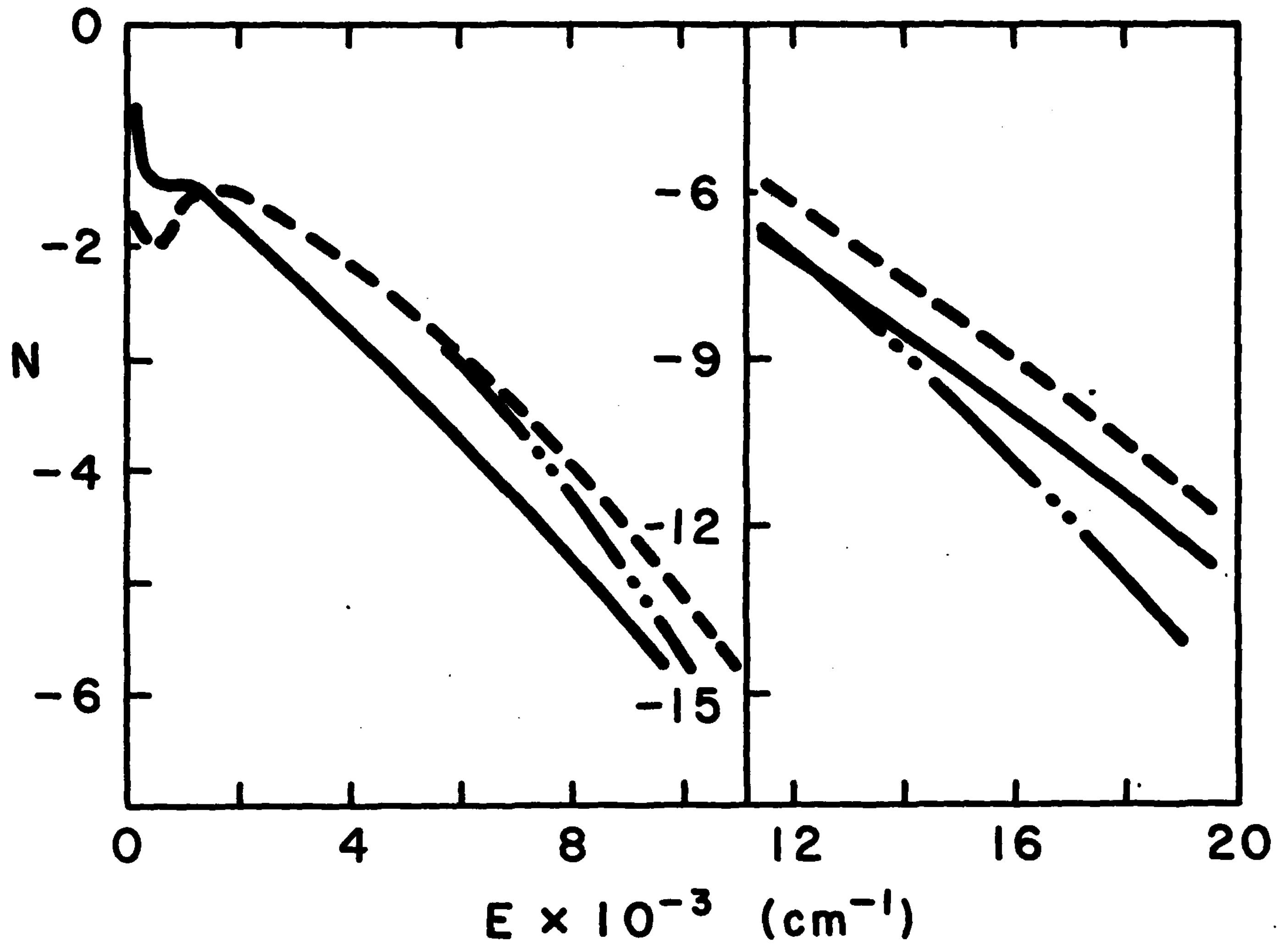
N
0
-2
-4
-6
-6
-9
-12
-15
0
4
8
12
16
20
E × 10^{-3} (cm^{-1})

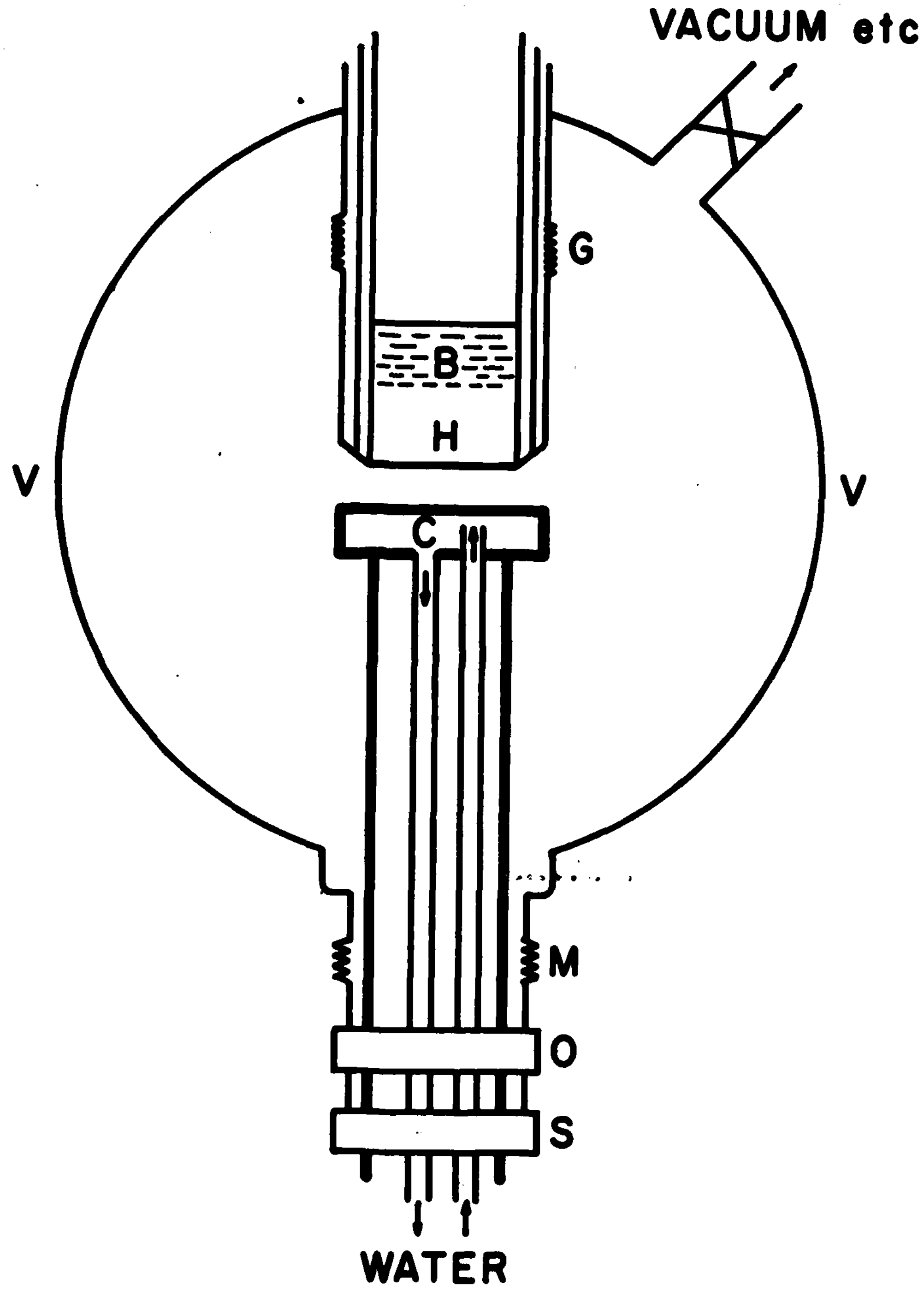
VACUUM etc
G
B
H
V
V
C
M
O
S
WATER

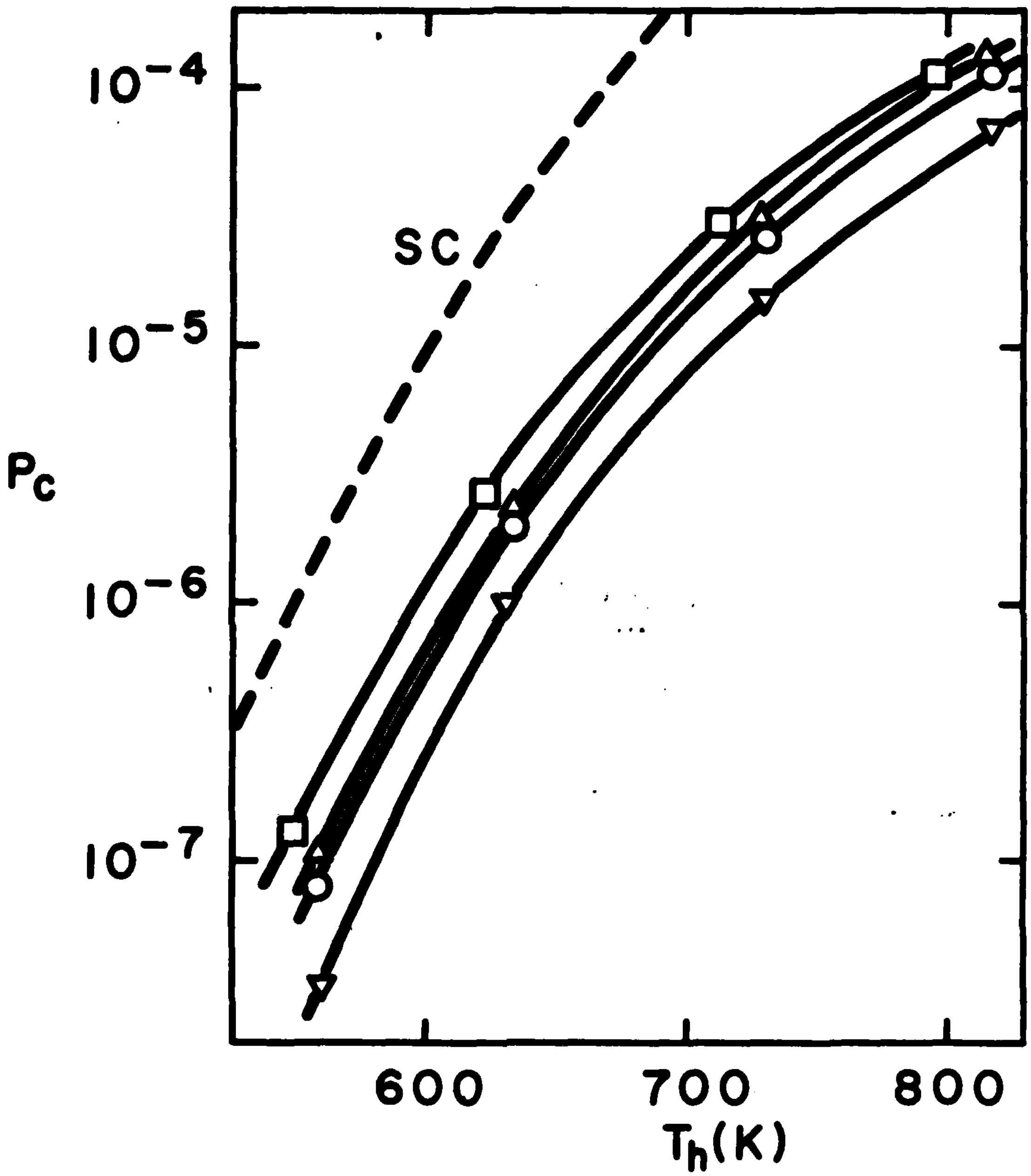
SC
Pc
10^{-4}
10^{-5}
10^{-6}
10^{-7}
600
700
800
$T_h(K)$

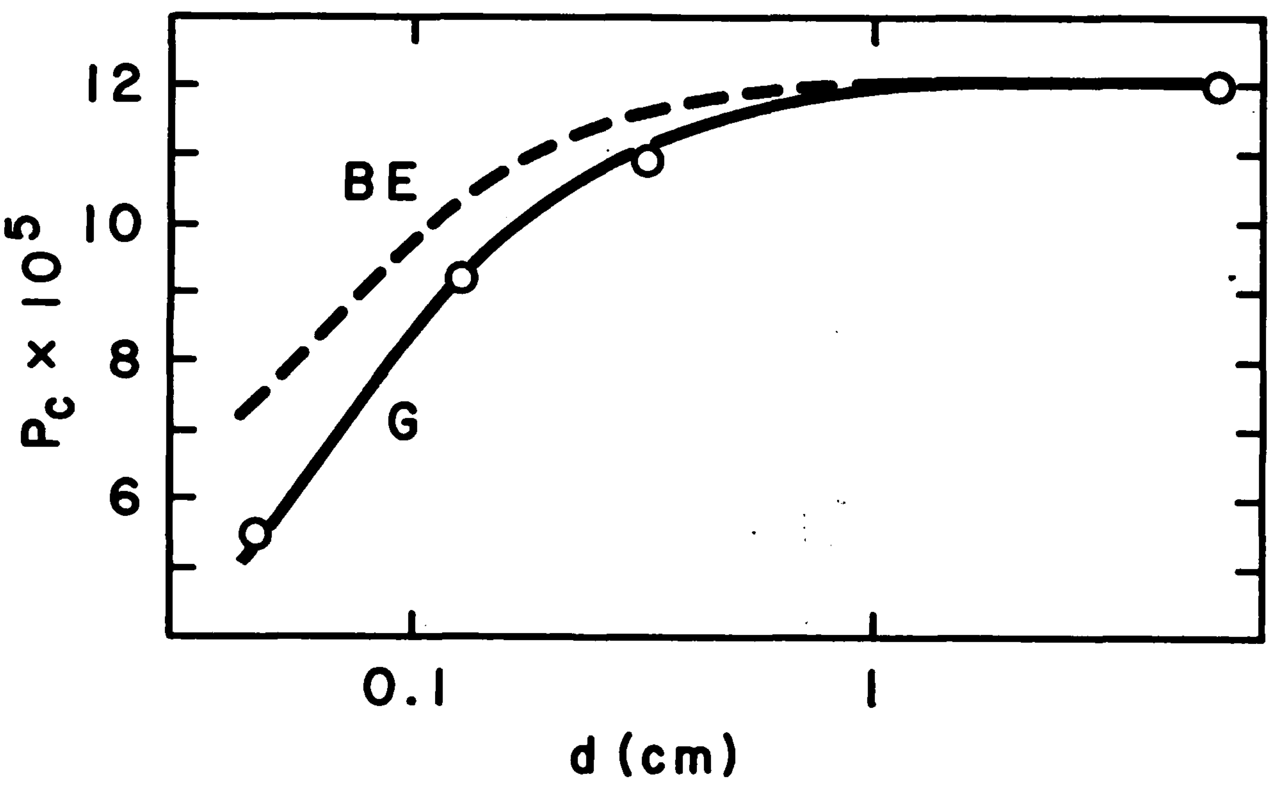
12
10
8
6
BE
G
$P_c \times 10^5$
0.1
1
d (cm)

INIT

DISTRIBUTION LIST

July 31, 1983

	No. Copies
Dr. L.V. Schmidt Assistant Secretary of the Navy (R,E, and S) Room 5E 731 Pentagon Washington, D.C. 20350	1
Dr. A.L. Slafkosky Scientific Advisor Commandant of the Marine Corps Code RD-1 Washington, D.C. 20380	1
Dr. Richard S. Miller Office of Naval Research Code 432 Arlington, VA 22217	10
Mr. David Siegel Office of Naval Research Code 260 Arlington, VA 22217	1
Dr. R.J. Marcus Office of Naval Research Western Office 1030 East Green Street Pasadena, CA 91106	1
Dr. Larry Peebles Office of Naval Research East Central Regional Office 666 Summer Street, Bldg. 114-D Boston, MA 02210	1
Dr. Phillip A. Miller Office of Naval Research Naval Station, Treasure Island Bldg. 7, Rm. 81 San Francisco, CA 94130	1
Mr. Otto K. Heiney AFATL - DLDL Eglin AFB, FL 32542	1
Mr. R. Geisler ATTN: MKP/MS24 AFRPL Edwards AFB, CA 93523	1
Dr. F. Roberto Code AFRPL MKPA Edwards AFB, CA 93523	1
Dr. L.H. Caveny Air Force Office of Scientific Research Directorate of Aerospace Sciences Bolling Air Force Base Washington, D.C. 20332	1
Mr. Donald L. Ball Air Force Office of Scientific Research Directorate of Chemical Sciences Bolling Air Force Base Washington, D.C. 20332	1
Dr. John S. Wilkes, Jr. FJSRL/NC USAF Academy, CO 80840	1
Dr. R.L. Lou Aerojet Strategic Propulsion Co. P.O. Box 15699C Sacramento, CA 95813	1
Dr. V.J. Keenan Anal-Syn Lab Inc. P.O. Box 547 Paoli, PA 19301	1
Dr. Philip Howe Army Ballistic Research Labs ARRADCOM Code DRDAR-BLT Aberdeen Proving Ground, MD 21005	1
Mr. L.A. Watermeier Army Ballistic Research Labs ARRADCOM Code DRDAR-BLI Aberdeen Proving Ground, MD 21005	1
Dr. W.W. Wharton Attn: DRSMI-RKL Commander U.S. Army Missile Command Redstone Arsenal, AL 35898	1

DISTRIBUTION LIST

	No. Copies
Mr. J. Murrin Naval Sea Systems Command Code 62R2 Washington, D.C. 20362	1
Dr. P.J. Pastine Naval Surface Weapons Center Code R04 White Oak Silver Spring, MD 20910	1
Mr. L. Roslund Naval Surface Weapons Center Code R122 White Oak Silver Spring, MD 20910	1
Mr. M. Stosz Naval Surface Weapons Center Code R121 White Oak Silver Spring, MD 20910	1
Dr. E. Zimmet Naval Surface Weapons Center Code R13 White Oak Silver Spring, MD 20910	1
Dr. D.R. Derr Naval Weapons Center Code 388 China Lake, CA 93555	1
Mr. Lee N. Gilbert Naval Weapons Center Code 3205 China Lake, CA 93555	1
Dr. E. Martin Naval Weapons Center Code 3858 China Lake, CA 93555	1
Mr. R. McCarten Naval Weapons Center Code 3272 China Lake, CA 93555	1
Dr. A. Nielsen Naval Weapons Center Code 385 China Lake, CA 93555	1
Dr. R. Reed, Jr. Naval Weapons Center Code 388 China Lake, CA 93555	1
Dr. L. Smith Naval Weapons Center Code 3205 China Lake, CA 93555	1
Dr. B. Douda Naval Weapons Support Center Code 5042 Crane, IN 47522	1
Dr. A. Faulstich Chief of Naval Technology MAT Code 0716 Washington, D.C. 20360	1
LCDR J. Walker Chief of Naval Material Office of Naval Technology MAT, Code 0712 Washington, D.C. 20360	1
Mr. Joe McCartney Naval Ocean Systems Center San Diego, CA 92152	1
Dr. S. Yamamoto Marine Sciences Division Naval Ocean Systems Center San Diego, CA 91232	1
Dr. G. Bosmajian Applied Chemistry Division Naval Ship Research & Development Center Annapolis, MD 21401	1
Dr. H. Shuey Rohm and Haas Company Huntsville, AL 35801	1

DISTRIBUTION LIST

	No. Copies
Mr. R. Brown Naval Air Systems Command Code 330 Washington, D.C. 20361	1
Dr. H. Rosenwasser Naval Air Systems Command AIR-310C Washington, D.C. 20360	1
Mr. B. Sobers Naval Air Systems Command Code 03P25 Washington, D.C. 20360	1
Dr. L.R. Rothstein Assistant Director Naval Explosives Dev. Engineering Dept. Naval Weapons Station Yorktown, VA 23691	1
Dr. Lionel Dickinson Naval Explosive Ordnance Disposal Tech. Center Code D Indian Head, MD 20640	1
Mr. C.L. Adams Naval Ordnance Station Code PM4 Indian Head, MD 20640	1
Mr. S. Mitchell Naval Ordnance Station Code 5253 Indian Head, MD 20640	1
Dr. William Tolles Dean of Research Naval Postgraduate School Monterey, CA 93940	1
Naval Research Lab. Code 6100 Washington, D.C. 20375	1

	No. Copies
Dr. J. Schnur Naval Research Lab. Code 6510 Washington, D.C. 20375	1
Mr. R. Beauregard Naval Sea Systems Command SEA 64E Washington, D.C. 20362	1
Mr. G. Edwards Naval Sea Systems Command Code 62R3 Washington, D.C. 20362	1
Mr. John Boyle Materials Branch Naval Ship Engineering Center Philadelphia, PA 19112	1
Dr. H.G. Adolph Naval Surface Weapons Center Code R11 White Oak Silver Spring, MD 20910	1
Dr. T.D. Austin Naval Surface Weapons Center Code R16 Indian Head, MD 20640	1
Dr. T. Hall Code R-11 Naval Surface Weapons Center White Oak Laboratory Silver Spring, MD 20910	1
Mr. G.L. Mackenzie Naval Surface Weapons Center Code R101 Indian Head, MD 20640	1
Dr. K.F. Mueller Naval Surface Weapons Center Code R11 White Oak Silver Spring, MD 20910	1

DISTRIBUTION LIST

No. Copies

Dr. R.G. Rhoades 1
Commander
Army Missile Command
DRSMI-R
Redstone Arsenal, AL 35898

Dr. W.D. Stephens 1
Atlantic Research Corp.
Pine Ridge Plant
7511 Wellington Rd.
Gainesville, VA 22065

Dr. A.W. Barrows 1
Ballistic Research Laboratory
USA ARRADCOM
DRDAR-BLP
Aberdeen Proving Ground, MD 21005

Dr. C.M. Frey 1
Chemical Systems Division
P.O. Box 358
Sunnyvale, CA 94086

Professor F. Rodriguez 1
Cornell University
School of Chemical Engineering
Olin Hall
Ithaca, NY 14853

Defense Technical Information Center 12
DTIC-DDA-2
Cameron Station
Alexandria, VA 22314

Dr. Ronald L. Simmons 1
Hercules Inc. Eglin
AFATL/DLDL
Eglin AFB, FL 32542

No. Copies

Dr. E.H. Debutts 1
Hercules Inc.
Baccus Works
P.O. Box 98
Magna, UT 84044

Dr. James H. Thacher 1
Hercules Inc. Magna
Baccus Works
P.O. Box 98
Magna, UT 84044

Mr. Theodore M. Gilliland 1
Johns Hopkins University APL
Chemical Propulsion Info. Agency
Johns Hopkins Road
Laurel, MD 20810

Dr. R. McGuire 1
Lawrence Livermore Laboratory
University of California
Code L-324
Livermore, CA 94550

Dr. Jack Linsk 1
Lockheed Missiles & Space Co.
P.O. Box 504
Code Org. 83-10, Bldg. 154
Sunnyvale, CA 94088

Dr. B.G. Craig 1
Los Alamos National Lab
P.O. Box 1663
NSP/DOD, MS-245
Los Alamos, NM 87545

Dr. R.L. Rabie 1
WX-2, MS-952
Los Alamos National Lab.
P.O. Box 1663
Los Alamos, NM 87545

Dr. R. Rogers 1
Los Alamos Scientific Lab.
WX-2
P.O. Box 1663
Los Alamos, NM 87545

6/81

DISTRIBUTION LIST

No. Copies

Dr. J.F. Kincaid 1
Strategic Systems Project
Office
Department of the Navy
Room 901
Washington, D.C. 20376

Strategic Systems Project Office 1
Propulsion Unit
Code SP2731
Department of the Navy
Washington, D.C. 20376

Mr. E.L. Throckmorton 1
Strategic Systems Project Office
Department of the Navy
Room 1048
Washington, D.C. 20376

Dr. D.A. Flanigan 1
Thiokol
Huntsville Division
Huntsville, AL 35807

Mr. G.F. Mangum 1
Thiokol Corporation
Huntsville Division
Huntsville, AL 35807

Mr. E.S. Sutton 1
Thiokol Corporation
Elkton Division
P.O. Box 241
Elkton, MD 21921

Dr. G. Thompson 1
Thiokol
Wasatch Division
MS 240 P.O. Box 524
Brigham City, UT 84302

Dr. T.F. Davidson 1
Technical Director
Thiokol Corporation
Government Systems Group
P.O. Box 9258
Ogden, UT 84409

No. Copies

Dr. C.W. Vriesen 1
Thiokol Elkton Division
P.O. Box 241
Elkton, MD 21921

Dr. J.C. Hinshaw 1
Thiokol Wasatch Division
P.O. Box 524
Brigham City, UT 83402

U.S. Army Research Office 1
Chemical & Biological Sciences
Division
P.O. Box 12211
Research Triangle Park, NC 27709

Dr. R.F. Walker 1
USA ARRADCOM
DRDAR-LCE
Dover, NJ 07801

Dr. T. Sinden 1
Munitions Directorate
Propellants and Explosives
Defense Equipment Staff
British Embassy
3100 Massachusetts Ave.
Washington, D.C. 20008

Mr. J.M. Frankle 1
Army Ballistic Research Labs
ARRADCOM
Code DRDAR-BLI
Aberdeen Proving Ground, MD 21005

Dr. Ingo W. May 1
Army Ballistic Research Lab
ARRADCOM
Code DRDAR-BLI
Aberdeen Proving Ground, MD 21005

DISTRIBUTION LIST

No. Copies

E. J. Palm 1
Commander
Army Missile Command
DRSMI-RK
Redstone Arsenal, AL 35898

Dr. Merrill K. King 1
Atlantic Research Corp.
5390 Cherokee Avenue
Alexandria, VA 22314

Dr. R.J. Bartlett 1
Batelle Columbus Laboratories
505 King Avenue
Columbus, OH 43201

Dr. P. Rentzepis 1
Bell Laboratories
Murray Hill, NJ 07971

Professor Y.T. Lee 1
Department of Chemistry
University of California
Berkeley, CA 94720

Professor M. Nicol 1
Department of Chemistry
405 Hilgard Avenue
University of California
Los Angeles, CA 90024

Professor S.S. Penner 1
University of California
Energy Center
Mail Code B-010
La Jolla, CA 92093

Professor Curt Wittig 1
University of Southern CA
Dept. of Electrical Engineering
University Park
Los Angeles, CA 90007

Dr. Kenneth O. Hartman 1
Hercules Aerospace Division
Hercules Incorporated
Allegany Ballistics Lab
P.O. Box 210
Cumberland, MD 21502

Dr. Joyce J. Kaufman 1
The Johns Hopkins University
Department of Chemistry
Baltimore, MD 21218

Dr. John K. Dienes 1
T-3, MS-216
Los Alamos National Lab
P.O. Box 1663
Los Alamos, NM 87544

Dr. H.P. Marshall 1
Dept. 52-35, Bldg. 204.2
Lockheed Missile & Space Co.
3251 Hanover Street
Palo Alto, CA 94304

Professor John Deutsch 1
MIT
Department of Chemistry
Cambridge, MA 02139

Professor Barry Kunz 1
College of Sciences & Arts
Department of PHysics
Michigan Technological Univ.
Houghton, MI 49931

Dr. R. Bernecker 1
Code R13
Naval Surface Weapons Center
White Oak
Silver Spring, MD 20910

Dr. C.S. Coffey 1
Naval Surface Weapons Center
Code R13
White Oak
Silver Spring, MD 20910

DISTRIBUTION LIST

No. Copies

Dr. W. L. Elban 1
Code R13
Naval Surface Weapons Center
White Oak
Silver Spring, MD 20910

Mr. K.J. Graham 1
Naval Weapons Center
Code 3835
China Lake, CA 93555

Dr. B. Junker 1
Office of Naval Research
Code 421
Arlington, VA 22217

Prof. H.A. Rabitz 1
Department of Chemistry
Princeton University
Princeton, NH 08540

Dr. M. Farber 1
Space Sciences, Inc.
135 West Maple Avenue
Monrovia, CA 91016

Mr. M. Hill 1
SRI International
333 Ravenswood Avenue
Menlo Park, CA 94025

U.S. Army Research Office 1
Engineering Division
Box 12211
Research Triangle Park, NC 27709

U.S. Army Research Office 1
Metallurgy & Materials Sci. Div.
Box 12211
Research Triangle Park, NC 27709

Professor G.D. Duvall 1
Washington State University
Department of Physics
Pullman, WA 99163